Full-band simulation of indirect phonon assisted tunneling in a silicon tunnel diode with delta-doped contacts

Cristian Rivas[a)]
Eric Jonsson School of Engineering, University of Texas at Dallas, Richardson, Texas 75083-0688

Roger Lake
Raytheon Systems, P.O. 660246, MS 35, Dallas, Texas 75266

Gerhard Klimeck
Jet Propulsion Laboratory, California Institute of Technology, MS Pasadena, California 91109-8099

William R. Frensley
Eric Jonsson School of Engineering, University of Texas at Dallas, Richardson, Texas 75083-0688

Massimo V. Fischetti
IBM Research Division, Thomas J. Watson Research Center, P.O. 218, Yorktown Heights, New York 10598

Phillip E. Thompson
Naval Research Laboratory, Washington, DC 20375-5347

Sean L. Rommel and Paul R. Berger
Department of Electrical and Computer Engineering, University of Delaware, Newark, Delaware 19716-3130

(Received 28 August 2000; accepted for publication 21 November 2000)

Full-band simulations of indirect, phonon assisted, interband tunneling are used to calculate the current–voltage response of a low-temperature molecular-beam-epitaxy-grown silicon tunnel diode with delta-doped contacts. Electron confinement in the contacts results in weak structure in the current–voltage characteristic. The structure is lost when finite lifetime effects are included. The approach uses the nonequilibrium Green function formalism in a second-neighbor $sp3s^*$ planar orbital basis. © *2001 American Institute of Physics.* [DOI: 10.1063/1.1343500]

Modern versions of the silicon interband tunnel diode fabricated with low-temperature molecular-beam epitaxy have recently been demonstrated in Si/Si_xGe_{1-x} and all Si devices.[1–8] One common feature of these tunnel diodes is their delta-doped[1–7] or heavily doped[8] contacts. The delta doping gives rise to potential wells on either side of the tunnel junction. The electron transport is an indirect ($X-\Gamma$), phonon assisted, interband tunneling process. It has not been understood how the potential wells in the contacts affect the current-voltage ($I-V$) response compared to that of a traditional tunnel diode with bulk doping in the contacts. If confined levels existed in the potential wells, one might expect to see structure in the $I-V$ as the levels uncross, but it was an open question as to where in the $I-V$ the structure would appear. It also seemed possible that the quasi-two-dimensional (2D) nature of the contacts might affect the magnitude of the current. In response to these questions, we present full-band calculations of indirect, phonon assisted tunneling. The results show where in the $I-V$ curve the structure occurs, how the magnitude of the current is affected, and how the structure is removed from finite lifetime effects.

Our approach uses the nonequilibrium Green function formalism with a second neighbor $sp3s^*$ planar orbital basis.[9–11] The $sp3s^*$ parameters are optimized using a genetic algorithm.[12] The Green function formalism allows us to model the finite lifetime in the quasi-2D contacts using the generalized boundary conditions described in Refs. 10 and 13.

The deformation potential phonon assisted tunneling current is given by the following expression:

$$J_1=\frac{e(D_tK)^2}{2\rho\omega a}\int\frac{d^2\mathbf{k}_{\mathcal{L}}}{4\pi^2}\int\frac{d^2\mathbf{k}_{\mathcal{R}}}{4\pi^2}\int\frac{dE}{2\pi}\sum_L\{tr[G^A_{L,1}(\mathbf{k}_{\mathcal{L}},E)\Gamma^{\mathcal{L}}_{1,1}(\mathbf{k}_{\mathcal{L}},E)G^R_{1,L}(\mathbf{k}_{\mathcal{L}},E)][f_{\mathcal{L}}(E)(1-f_{\mathcal{R}}(E-\hbar\omega))(n_B(\hbar\omega)+1)$$
$$\times trA^{\mathcal{R}}_L(\mathbf{k}_{\mathcal{R}},E-\hbar\omega)+f_{\mathcal{L}}(E)(1-f_{\mathcal{R}}(E+\hbar\omega))n_B(\hbar\omega)trA^{\mathcal{R}}_L(\mathbf{k}_{\mathcal{R}},E+\hbar\omega)-(1-f_{\mathcal{L}}(E))f_{\mathcal{R}}(E-\hbar\omega)n_B(\hbar\omega)$$
$$\times trA^{\mathcal{R}}_L(\mathbf{k}_{\mathcal{R}},E-\hbar\omega)-(1-f_{\mathcal{L}}(E))f_{\mathcal{R}}(E+\hbar\omega)(n_B(\hbar\omega)+1)trA^{\mathcal{R}}_L(\mathbf{k}_{\mathcal{R}},E+\hbar\omega)]\}, \quad (1)$$

a)Electronic mail: cor2282@utdallas.edu

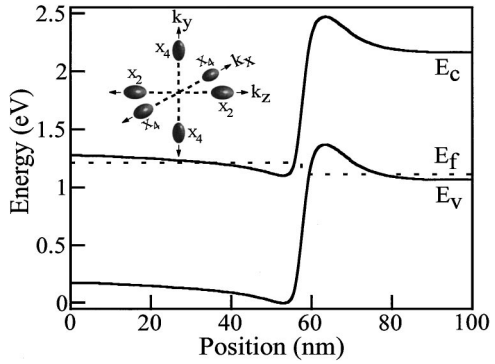

FIG. 1. Band profile and quasi-Fermi level for RITD biased at 0.1 V. Inset, 6 X valleys of the conduction band.

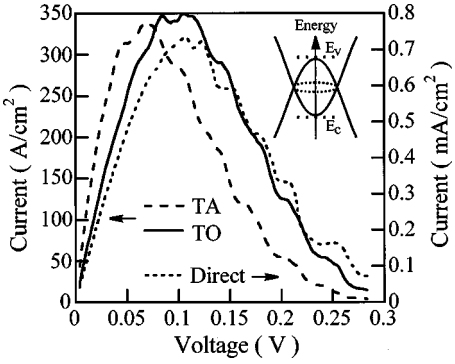

FIG. 2. Three RITD current components: TA phonon assisted, TO phonon assisted, and direct. The scattering lifetime in the contacts is 165 fs. Inset, 2D electron and hole dispersions.

where $A_L^{\mathcal{R}}$ is the component of the spectral function injected from the right contact

$$A_L^{\mathcal{R}}(\mathbf{k}_{\mathcal{R}},E)=G_{L,N}^{R}(\mathbf{k}_{\mathcal{R}},E)\Gamma_{N,N}^{\mathcal{R}}(\mathbf{k}_{\mathcal{R}},E)G_{N,L}^{A}(\mathbf{k}_{\mathcal{R}},E). \quad (2)$$

Equation (1) is Fermi's Golden Rule in Green function form calculating the overlap of the wave function envelopes. The subscript or superscript $\mathcal{L}$ and $\mathcal{R}$ indicate that the quantity is injected from the left or right contact, respectively. The wave vectors $\mathbf{k}_{\mathcal{L}}$ and $\mathbf{k}_{\mathcal{R}}$ are transverse, two-dimensional wave vectors in the $x-y$ plane. E is the total energy. The sum over L is a sum over monolayers in the growth direction lying within the nonequilibrium region indexed left to right from 1 to N. Γ is obtained from the surface Green functions of the contact regions,[10] G^R and G^A are the retarded and advanced Green functions, respectively, $tr\{\ \}$ indicates a trace over the 20 orbitals in the sp^3s^* basis, $f_{\mathcal{L}}$ and $f_{\mathcal{R}}$ are the Fermi factors of the left and right contacts, respectively, ω is the phonon frequency, $n_B(\hbar\omega)$ is the Bose-Einstein factor, ρ is the density of Si, 2.328 g/cm^3, a is the lattice parameter, 5.431 Å, and D_tK is the interband deformation potential.

Equation (1) is calculated independently for each phonon type. The direct tunneling current from the two longitudinal X valleys of the conduction band (the two valleys labeled X_2 in the inset of Fig. 1) to the Γ valley of the valence band is also calculated using the approach described in Ref. 10.

Two different phonons provide the main contribution to the current, the transverse acoustic (TA) phonon with an energy of 18.4 meV and the transverse optical (TO) phonon with an energy of 57.6 meV.[14] Using the simplest deformation potential concept, and values from Ref. 15, one can estimate a value of D_tK for the interband (100) TA phonon to be 2.45×10^8 eV/cm. There exists no similar method to estimate the matrix element for the TO phonon. However, we know experimentally that the contribution to the total current from the TA and TO phonons is almost equal.[16] We use this fact to estimate a value of D_tK for the TO phonon by comparing the two numerically calculated current contributions. We estimate the value to be 5.6×10^8 eV/cm.

The band diagram shown in Fig. 1 of the Silicon tunnel diode reported in Ref. 4 is calculated from Poisson's equation using the secondary ion mass spectroscopy (SIMS) doping profile measured after a 700 °C rapid thermal anneal assuming complete dopant activation.[4] All calculations use a temperature of 300 K. Because of the confinement in the δ-doped contacts, we will refer to this device as a resonant interband tunnel diode (RITD).[1] To compare the calculated $I-V$ of this device with a traditional tunnel diode with bulk-like contacts, which we will refer to as an Esaki diode, we modify the band profile shown in Fig. 1 by attaching flat-bands at the deepest point in the electron well and the highest point in the hole potential well. Thus, the deep wells are replaced with equivalently deep three-dimensional regions. This comparison can be viewed as a numerical *gedanken* experiment since the delta doping is used precisely for the reason that equivalently heavy bulk doping has not yet been achieved.

To observe the structure in the RITD $I-V$ and its disappearance with finite lifetime broadening, the RITD contacts are modeled using five different values for the scattering lifetime resulting from the heavy doping: 165, 66, 33, 7.3, and 4.3 fs. The measured Hall mobility in the Sb-doped well is 30 cm^2/V s[17] which, using the relation $\mu=e\tau/m^*$, results in an estimate for τ of 4.3 fs. The Esaki diode is modeled with the 165 fs lifetime.

The calculated components of the RITD $I-V$ with the 165 fs lifetime are shown in Fig. 2. Note that the axis for the direct current is in units of mA/cm^2, whereas the axis for the phonon assisted components is in units of A/cm^2. The direct component of the current is approximately five orders of magnitude smaller than the phonon assisted components. Low-temperature measurements made on similar devices[18] show that the ratio is significantly larger than that observed in the alloyed tunnel diodes of the 1960s;[16] however, it does not appear to be more than two orders of magnitude. The discrepancy could be the result of elastic intervalley scattering processes which are not included in these simulations.

Structure is observed in the $I-V$ components, most noticeably in the negative differential resistance (NDR) region. This is different than that observed for intraband 2D-2D tunneling where the features occur on the positive differential section of the $I-V$ curve (compare, for example, Fig. 4 of Ref. 13). Roughly speaking, the difference lies in the fact that the quantized states are the bottom of 2D subbands which are now inverted from each other as illustrated in the inset of Fig. 2.

The total currents for the Esaki diode and the RITDs with contact lifetimes of 165, 33, 7.3, and 4.3 fs are shown in Fig. 3. The 66 fs RITD is left out for clarity. Weak structure appears in the 165 and 66 fs RITD $I-V$s. Some cancellation

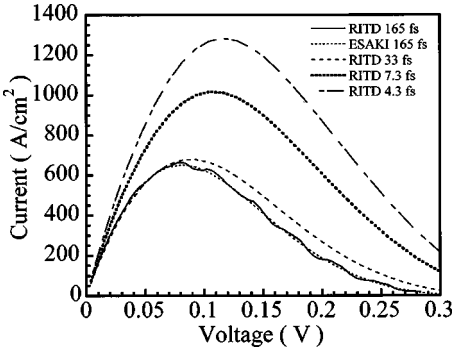

FIG. 3. Total current for the Esaki diode and the RITDs with contact scattering lifetimes as labeled.

of the structure found in the individual components occurs when they are added. No structure is observed in the 33, 7.3, and 4.3 fs RITD $I-V$s. The 165 fs RITD $I-V$ fluctuates around the smooth 165 fs Esaki diode $I-V$. As the contact lifetime decreases, the current magnitude and peak voltage increase. To show clearly where the structure occurs in the RITD $I-V$s, Fig. 4 displays the first derivative of the 165 and 66 fs RITD $I-V$s.

Last, we compare the simulated peak current and voltage with the experimental data. When the experimental $I-V$ is corrected for series resistance, the experimental peak voltage is approximately 100 mV and the peak current is 7000 A/cm^2. The simulated peak voltage ranges between 80 and 115 mV from the longest to the shortest contact lifetimes, and the simulated peak current ranges between 650 and 1275 A/cm^2. There are several factors which affect the calculated current density. The current is directly proportional to the square of the deformation potentials for which we made a rough estimate. The actual dopant distributions are sharper than the SIMS profiles. The current will have an exponential dependence on the accuracy of the evanescent dispersion at X and Γ. These uncertainties and the exponential dependence of tunneling current on material parameters

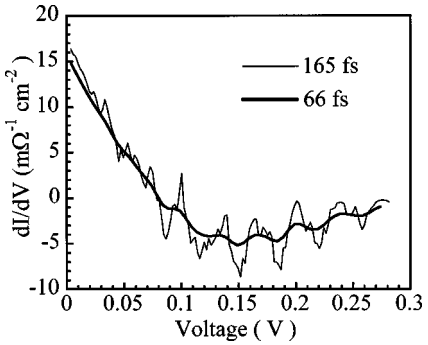

FIG. 4. First derivative of the RITD $I-V$s with 165 and 66 fs contact scattering lifetimes.

and geometry can account for the discrepancy in the calculated and experimental current.

In conclusion, we have presented simulations of traditional Si tunnel diodes and RITDs using modern full-band quantum device modeling methods. The quasi-2D nature of δ-doped contacts gives rise to weak structure in the current-voltage curve mostly in the NDR region. However, the structure quickly disappears when realistic finite lifetime effects are included in the contacts.

This work was partially supported by DARPA/AFOSR and the Texas Advanced Technology Program under Grant No. 036327-074. The authors gratefully thank David Simons for providing the SIMS data and Dave Surina and Mark Kimmons for making available to the authors Raytheon's 28 CPU Origin 2000. Also invaluable is the extensive computer time, used for tight binding parameter generation and numerous preliminary test runs, on various systems provided by the Jet Propulsion Laboratory, California Institute of Technology under a contract with the National Aeronautics and Space Administration. The supercomputer used in these investigations at JPL was provided by funding from the NASA Offices of Earth Science, Aeronautics, and Space Science.

[1] S. L. Rommel, T. E. Dillon, M. W. Dashiell, H. Feng, J. Kolodzey, P. R. Berger, P. E. Thompson, K. D. Hobart, R. Lake, A. Seabaugh, G. Klimeck, and D. K. Blanks, Appl. Phys. Lett. **73**, 2191 (1998).
[2] S. L. Rommel, T. E. Dillon, P. R. Berger, R. Lake, P. E. Thompson, K. D. Hobart, A. C. Seabaugh, and D. S. Simmons, in *1998 IEDM Technical Digest* (IEEE, New York, 1998), p. 1035.
[3] S. L. Rommel, T. E. Dillon, P. R. Berger, P. E. Thompson, K. D. Hobart, R. Lake, and A. Seabaugh, IEEE Electron Device Lett. **20**, 329 (1999).
[4] P. E. Thompson, K. D. Hobart, M. E. Twigg, G. G. Jernigan, T. E. Dillon, S. L. Rommel, P. R. Berger, D. S. Simons, P. H. Chi, R. Lake, and A. Seabaugh, Appl. Phys. Lett. **75**, 1308 (1999).
[5] R. Duschl, O. G. Schmidt, G. Reitemann, E. Kasper, and K. Eberl, Electron. Lett. **35**, 1111 (1999).
[6] R. Duschl, O. G. Schmidt, and K. Eberl, Appl. Phys. Lett. **76**, 879 (2000).
[7] R. Duschl, O. G. Schmidt, and K. Eberl, Physica E (Amsterdam) **7**, 836 (2000).
[8] M. W. Dashiell, R. T. Troeger, S. L. Rommel, T. N. Adam, P. R. Berger, J. K. C. Guedj, A. C. Seabaugh, and R. Lake, IEEE Trans. Electron Devices **47**, 1707 (2000).
[9] C. Caroli, R. Combescot, P. Nozieres, and D. Saint-James, J. Phys. C **5**, 21 (1972).
[10] R. Lake, G. Klimeck, R. C. Bowen, and D. Jovanovic, J. Appl. Phys. **81**, 7845 (1997).
[11] T. B. Boykin, Phys. Rev. B **54**, 8107 (1996).
[12] G. Klimeck, R. C. Bowen, T. B. Boykin, C. Salazar-Lazaro, T. A. Cwik, and A. Stoica, Superlattices Microstruct. **27**, 77 (2000).
[13] G. Klimeck, R. Lake, R. C. Bowen, W. R. Frensley, and T. Moise, Appl. Phys. Lett. **67**, 2539 (1995).
[14] A. G. Chynoweth, R. A. Logan, and D. E. Thomas, Phys. Rev. **125**, 877 (1962).
[15] M. V. Fischetti and S. E. Laux, J. Appl. Phys. **80**, 2234 (1996).
[16] R. A. Logan and A. G. Chynoweth, Phys. Rev. **131**, 89 (1963).
[17] P. E. Thompson, K. D. Hobart, M. E. Twigg, S. L. Rommel, N. Jin, P. R. Berger, R. Lake, A. C. Seabaugh, P. H. Chi, and D. S. Simons, Thin Solid Films (accepted).
[18] S. L. Rommel, Ph.D. thesis, University of Delaware, Newark, 2000.